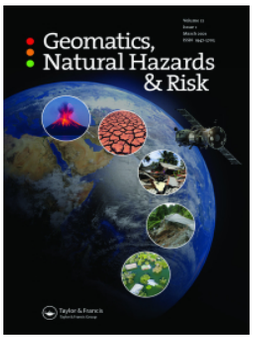

Geomatics, Natural Hazards and Risk

ISSN: 1947-5705 (Print) 1947-5713 (Online) Journal homepage: www.tandfonline.com/journals/tgnh20

Decadal trends analysis of extreme high temperatures and case simulation assessment in summer over Eastern China

Xuemin Shen , Aixia Feng , Changgui Gu & Qiguang Wang

To cite this article: Xuemin Shen , Aixia Feng , Changgui Gu & Qiguang Wang (2025) Decadal trends analysis of extreme high temperatures and case simulation assessment in summer over Eastern China, Geomatics, Natural Hazards and Risk, 16:1, 2526691, DOI: 10.1080/19475705.2025.2526691

To link to this article: https://doi.org/10.1080/19475705.2025.2526691

Published online: 06 Jul 2025.

GEOMATICS, NATURAL HAZARDS AND RISK
2025, VOL. 16, NO. 1, 2526691
https://doi.org/10.1080/19475705.2025.2526691

Decadal trends analysis of extreme high temperatures and case simulation assessment in summer over Eastern China

Xuemin Shen[a], Aixia Feng[b], Changgui Gu[a] and Qiguang Wang[c]

[a]Business School, University of Shanghai for Science and Technology, Shanghai, China; [b]National Meteorological Information Center, China Meteorological Administration, Beijing, China; [c]China Meteorological Administration Training Center, China Meteorological Administration, Beijing, China

ABSTRACT

Using the daily maximum temperature from the 0.5° × 0.5° grid datasets (V2.0) covering China during 1961–2020, this study conducts a decadal-scale spatio-temporal analysis of summer daily maximum temperatures across eastern China (east of 110°E, excluding Inner Mongolia and Northeast China). The results indicate that daily maximum temperatures during the summer months (June–August) exhibited a significant warming trend across three statistical measures—minimum, mean, and maximum values. The minimum temperature showed the most pronounced increase, rising by over 2 °C in the past six decades and accompanied by a broader temperature distribution. This trend was especially evident in central and eastern regions, indicating a marked intensification in both the frequency and severity of extreme heat events. Additionally, the study evaluated the performance of four operational forecasting models—CMA, ECMWF, NCEP, and UKMO—which participate in the Subseasonal to Seasonal (S2S) Prediction Project. The assessment found that short-term forecasts (1–10 days) had relatively small biases and high accuracy. UKMO is more reliable for short-term applications, while ECMWF shows greater potential for extended-range forecasting. In terms of heatwave prediction, all four models performed well at the 5-day lead time, with CMA producing the most accurate forecasts.

ARTICLE HISTORY
Received 9 July 2024
Accepted 23 June 2025

KEYWORDS
Extreme high temperature; heatwave; variation of trend; spatio-temporal distribution; model evaluation

1. Introduction

The Intergovernmental Panel on Climate Change (IPCC) released the Working Group I report, 'Climate Change 2021: The Physical Science Basis', in August 2021. This report indicates that since 1970, the rising rate of surface temperature globally has been faster than during any 50-year period over the past 2000 years (Shi 2012; Lu et al. 2022). Among all countries, China stands out as a region significantly sensitive

CONTACT Qiguang Wang wangqg@cma.gov.cn

to and impacted by global climate change, with a temperature increase rate notably higher than the global average during the same period. The increase of two major disastrous weather events in China (Ding and Qian 2011), high temperatures and subsequent heatwaves, has drawn widespread attention from scholars (Zhai and Pan 2003; Lin and Guan 2008; Sun et al. 2011; Li et al. 2015; Dong and Wu 2019; Xie et al. 2020). From 1951 to 2020, its annual average surface temperature has risen at a rate of 0.26 °C per decade. Studies have found that the number of extremely hot days in China on average has increased by about 8.5%, with the eastern and northwestern regions experiencing more intense heat (Sun et al. 2014; Yu and Sun 2019). The eastern part of China, situated within the East Asian monsoon region, is flanked by the Pacific Ocean to the east and the Qinghai-Tibet Plateau to the west, which to a certain extent contributes to its complex and varied climate system. And it is densely populated, mainly flat in terrain, and predominantly covered by farmland, making it one of the important centers for agricultural and economic development (Jiang 2021; Long 2022). Therefore, studying such extreme heat events over Eastern China under the global warming can provide crucial information for early warning and mitigating the negative impacts (Wang 2020).

Frequent heatwaves have impacts on natural ecosystems and human health. In order to reduce their negative effects, scientists aim to accurately predict their occurrence to implement emergency mitigation measures promptly. It is crucial to predict the heatwaves with a lead time exceeding 10 days, while the processes of physical mechanisms underlying medium-range and long-range weather forecasting still present numerous unresolved issues because of many objective constraints, making it challenging to both research and operation (Yang 2008; Hu et al. 2020). To advance the understanding on the sub-seasonal to seasonal time scale and improving forecast skill of extreme events, the World Weather Research Programme and the World Climate Research Programme jointly established the Sub-seasonal to Seasonal (S2S) Prediction Project. A key output of this project is the creation of a database containing reforecast and real-time ensemble forecast provided by 11 global operational meteorological agencies, which can be utilized to evaluate the capabilities of predicting extreme climate events among models participating in the S2S project. There is still a significant research gap in domestic researches on the predictability of heatwave occurrences using S2S models at present. Some research found that capturing seasonal oscillations in circulation anomalies was difficult for ECMWF model, which resulting in limited skill within a two-week lead time, through evaluating the forecasting ability of this model for the 2012 heatwave event in the Yangtze River Basin (Qi and Yang 2019). In the following year, another research evaluate three S2S models (ECMWF, CMA and NCEP) and identify the key factors affecting the sub-seasonal predictability of heatwaves in the same place (Xie et al. 2020). However, research on S2S models in Eastern China is currently limited and mostly focused on precipitation forecasting (He 2020; Wang and Li 2022), leaving a notable deficiency. Therefore, this study aims to evaluate the capability of four S2S models (CMA, ECMWF, NCEP, and UKMO) in forecasting daily maximum temperatures and heatwave events over eastern China during the summer of 2022. The evaluation focuses on multiple lead times (from 1 to 40 days), examining both the spatial and temporal prediction skill as

well as the bias and accuracy of each model. Prior to this, the study also conducts a long-term temporal and spatial analysis of summer temperature trends from 1961 to 2022 to establish a background understanding of the regional climate context. The findings enhance understanding of sub-seasonal forecast skill and offer support for improving model-based early warning systems for extreme heat events.

2. Data and method

2.1. Data

The dataset used in this study is derived from the $0.5^\circ \times 0.5^\circ$ gridded daily surface temperature dataset (V2.0) compiled by the National Meteorological Information Center of China. This dataset was constructed using thin plate spline (TPS) interpolation, integrating three-dimensional geographic information and based on observations from 2,472 surface weather stations across mainland China (excluding the offshore island stations of Xisha and Coral). Notably, data from Taiwan Province are not included. The analysis focused on daily maximum temperatures during the summer months (June to August) from 1961 to 2022. For model validation, real-time subseasonal-to-seasonal (S2S) forecast data of daily maximum temperatures from June to August 2022 were employed, produced by the European Centre for Medium-Range Weather Forecasts (ECMWF), the National Centers for Environmental Prediction (NCEP), United Kingdom Meteorological Office (UKMO), and the China Meteorological Administration (CMA). These forecast data were obtained from ECMWF | S2S, ECMWF, Realtime, Instantaneous and Accumulated.

2.2. Method

2.2.1. Definition of anomaly and heatwave

When analyzing the case of 2022, the extremity of the climate conditions was highlighted through the calculation of anomalies in daily maximum temperatures. Anomaly refers to the deviation of a meteorological variable from its standard climatological normals, and can be either positive or negative. According to the World Meteorological Organization (WMO), standard climatological normals is defined as the average of a given variable over the most recent three complete decades, representing the long-term mean state of that variable in a specific region. These reference periods are updated every ten years. For instance, the mean of 1961–1990 serves as the climate standard for the period 1991–2000. Accordingly, this study adopts the 30-year average from 1991 to 2020 as the reference.

For heatwave, there is no universally accepted standard for defining it currently (Ding et al. 2010; Perkins and Lewis 2020). Different studies propose various definitions; however, it is generally agreed that heatwaves represent periods of sustained elevated temperatures (Perkins 2015). This study adopts the widely used relative threshold method for defining heatwaves, identifying a heatwave at a given grid point as a period of three or more consecutive days with daily maximum temperatures at or above the 90th percentile of the temperature series (Alexander et al. 2006; Perkins et al. 2012; Stefanon et al. 2012; Zhang 2021).

2.2.2. The metrics for evaluation

For the evaluation of S2S model, the anomaly correlation coefficient (ACC) and temporal correlation coefficient (TCC) are used to respectively evaluate the similarity of the spatial distribution and temporal evolution between the prediction and observation. The root-mean-square error (RMSE) estimates the amplitude biases of prediction, for which smaller values indicate a better fit and lower error. The specific definitions of these evaluation metrics are as follows (Xie et al. 2020):

$$ACC(l,t) = \frac{\sum_{j=1}^{M}\sum_{i=1}^{N}\left\{\left(obs_{t,i,j} - \overline{obs_{i,j}}\right)\left(ref_{l,t,i,j} - \overline{ref_{l,i,j}}\right)\right\}}{\sqrt{\sum_{j=1}^{M}\sum_{i=1}^{N}\left(obs_{t,i,j} - \overline{obs_{i,j}}\right)^2 \sum_{j=1}^{M}\sum_{i=1}^{N}\left(ref_{l,t,i,j} - \overline{ref_{l,i,j}}\right)^2}} \tag{1}$$

$$TCC(l,i,j) = \frac{\frac{1}{T}\sum_{t=1}^{T}\left(obs_{t,i,j} - \overline{obs_{i,j}}\right)\left(ref_{l,t,i,j} - \overline{ref_{l,i,j}}\right)}{\sqrt{\frac{1}{T}\sum_{t=1}^{T}\left(obs_{t,i,j} - \overline{obs_{t,i,j}}\right)^2}\sqrt{\frac{1}{T}\sum_{t=1}^{T}\left(ref_{l,t,i,j} - \overline{ref_{l,i,j}}\right)^2}} \tag{2}$$

$$RMSE(l,i,j) = \sqrt{\frac{1}{T}\sum_{t=1}^{T}\left(ref_{l,t,i,j} - obs_{t,i,j}\right)^2} \tag{3}$$

where $obs_{t,i,j}$ represents the observed temperature, $ref_{l,t,i,j}$ represents the modeled temperature, t denotes a specific time, i and j represent specific latitude and longitude, l denotes the period validity, and M, N, T represent the total number of longitudes, latitudes, and times, respectively.

The categorical verification score known as the Heidke Skill Score (HSS) serves as the metric to evaluate the hit rate of heatwave days (P. Heidke 1926), which is defined as follows:

$$HSS = \frac{2(ad - bc)}{(a+c)(c+d) + (a+b)(b+d)} \tag{4}$$

where a represents the number of observed heatwave days that are correctly predicted, b is the number of false alarms, c represents the observed heatwave days that are not predicted, and d is the number of correct rejections. HSS ranges from $-\infty$ to 1. A negative value indicates that the random forecast is better, while a value of zero means no skill. A perfect prediction obtains an HSS value of 1.

2.2.3. Reconstruction of model's data

The forecast products from UKMO and NCEP are initialized daily, whereas those from CMA and ECMWF are issued twice weekly, specifically on Mondays and Thursdays. To facilitate a consistent comparison of forecast performance among the four models, a data reconstruction method proposed in previous studies (Yang et al. 2018; Qi and Yang 2019; Xie 2021) was applied to convert the twice-weekly forecasts into a daily format. This method uses forecast data from lead times $N-2$ to

$N + 2$ days to represent the forecast for day N. If two forecast values are available for a given lead time, their arithmetic mean is used. The comparison between the original and reconstructed forecast data at a one-day lead time from CMA and ECMWF (Figure 1) revealed similar distributions, indicating that the reconstruction process does not significantly affect the conclusions regarding forecast skill.

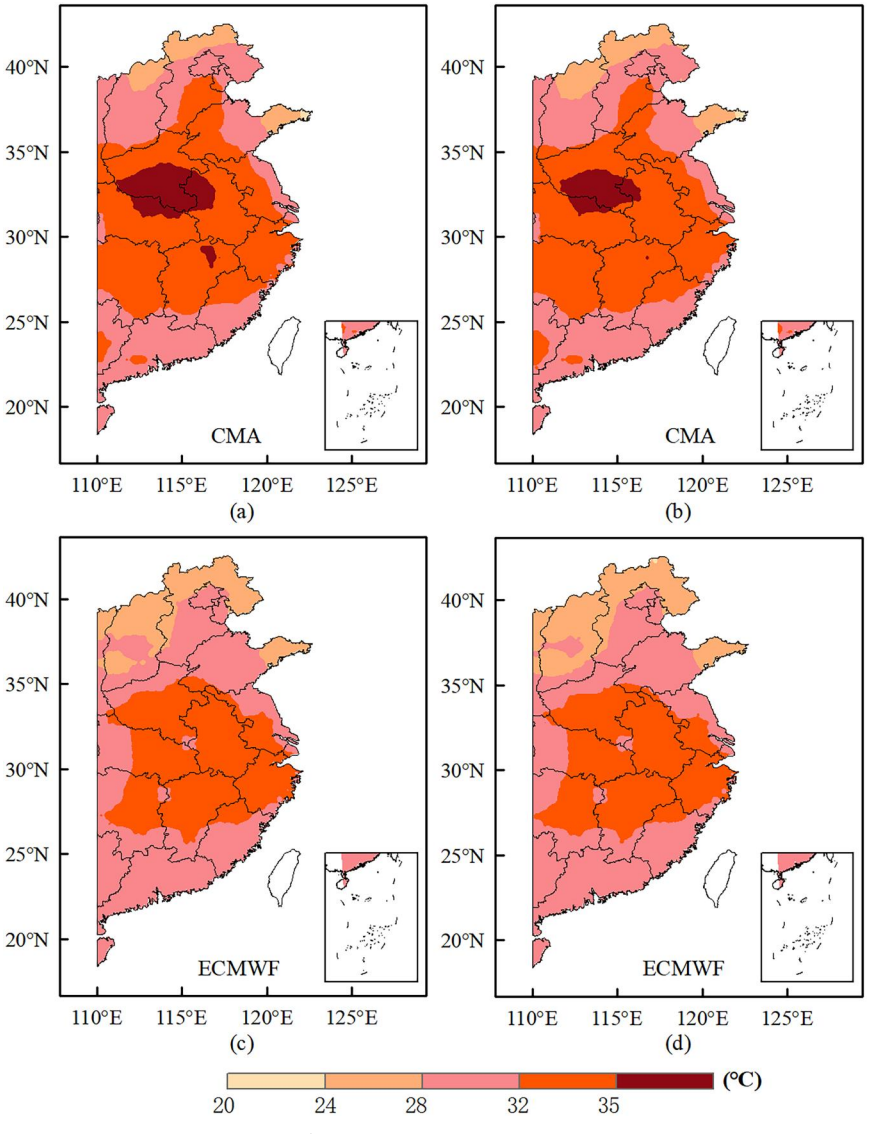

Figure 1. The spatial distribution of temperature predicted by CMA and ECMWF with the lead time of 1-day. (a) and (c) are original data, (b) and (d) are reconstructed data.

3. Results

3.1. Decadal analysis of high temperatures over Eastern China from 1961 to 2020

Figure 2 illustrates the decadal variation in three statistical characteristics of summer (June–August) daily maximum temperatures across China over the period 1961–2020. The analysis focuses on the minimum, mean, and maximum values within each decade. The minimum values show a clear warming tendency in recent decades. While the 1970s and 1980s exhibit weak or negative trends, a shift toward sustained warming begins in the 1990s, culminating in a pronounced increase during 2011–2020. The mean values remain relatively stable in the earlier periods, with only slight variations in slope. And a more evident upward trend emerges in the most recent decade. In contrast, the maximum values exhibit greater decadal variability. An increase in the 1980s is followed by a decline in the 2000s and a near-stable pattern in the 2010s.

The spatial distribution of three statistical measures of daily maximum temperature—minimum, mean, and maximum—during the summer months (June to August) across China for six consecutive decades is displayed in Figure 3. Over the past six decades, the minimum values of daily maximum temperature have shown a clear upward trend. In the earlier decades, minimum values were relatively low across

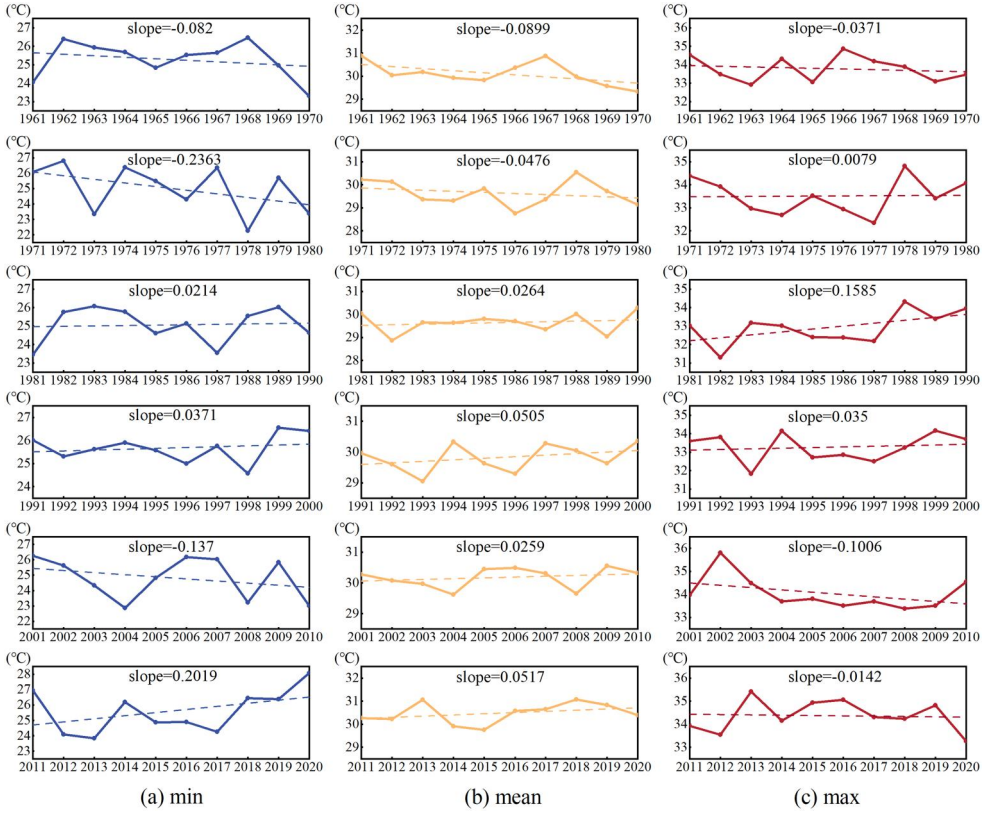

Figure 2. Decadal trend of (a) minimum, (b) mean, (c) maximum of daily maximum temperature in summer from 1961 to 2020.

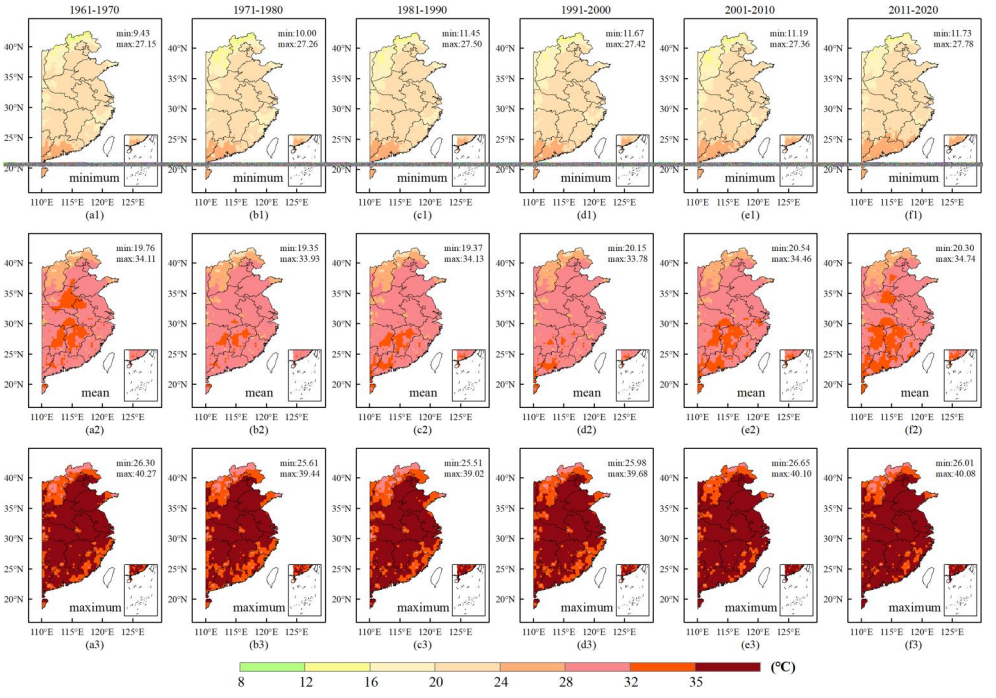

Figure 3. Decadal spatial distributions of (a) minimum, (b) mean, (c) maximum of daily maximum temperature in summer from 1961 to 2020.

most areas. By 2011–2020, a marked increase had occurred, with values rising from 9.43 °C to 11.73 °C—an increase of more than 2 °C. The mean values of daily maximum temperature exhibit a comparable warming pattern. While previous decades experienced relatively moderate mean temperatures, the 2011–2020 period is characterized by widespread warming, with many regions recording values exceeding 30 °C. The spatial distribution of the mean values closely resembles that of the minimum, with elevated temperatures concentrated in southern and eastern areas. The maximum values reveal an even more pronounced warming trend. In the most recent decade, daily maximum temperatures have surpassed 35 °C in the vast majority of areas, indicating a substantial intensification of extreme heat events in both frequency and magnitude.

In summary, the spatial and temporal patterns indicate that summer daily maximum temperatures have increased steadily over the past 60 years. All three statistical measures—minimum, mean, and maximum—reflect this warming trend, suggesting not only a general rise in summertime heat but also an enhancement in the frequency and severity of extreme heat events.

While the preceding analysis demonstrates the overarching warming trend, a month-by-month examination further elucidates the nuanced spatiotemporal patterns. Figure 4 reveals both shared and distinct characteristics in the distribution of daily maximum temperatures for June, July, and August across six decades from 1961 to 2020. Across all three months, a general warming trend is evident, with the median temperatures gradually increasing over time. The 2011–2020 period consistently

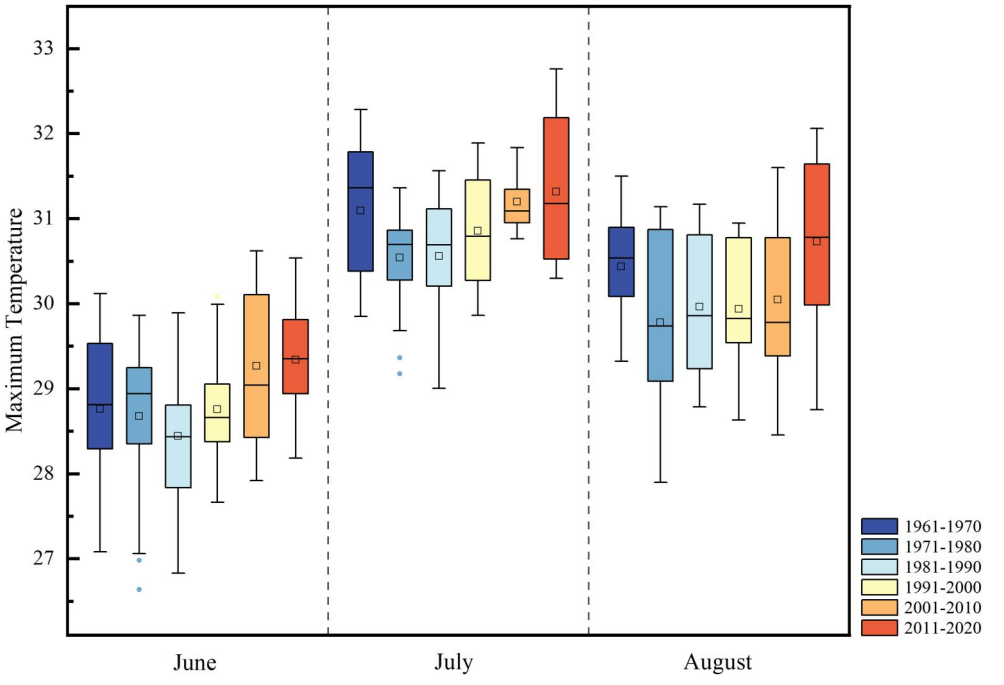

Figure 4. Box plot of decadal maximum temperature for each month from June to August.

shows the widest distribution of temperatures, suggesting increased variability and a higher likelihood of extreme values. From June to August, average daily maximum temperatures exhibit a clear seasonal progression, with June being relatively cooler (around 29 °C), July peaking at approximately 30 °C, and August showing a slight decline but still maintaining high values, generally between 29 °C and 30 °C. Across all three months, the 2011–2020 decade stands out with a notably wider temperature distribution, suggesting increased intra-month variability and a higher frequency of extreme temperature events in recent years.

The spatial distribution of daily maximum temperatures for June, July, and August across six decades from 1961 to 2020 is illustrated by Figure 5. Common features across all three months include a clear interdecadal warming trend and an expansion in the spatial extent of high-temperature areas, particularly in central and eastern regions. The temperature range has gradually shifted toward higher values, especially during the most recent decade (2011–2020). Overall, the spatial patterns indicate an interdecadal increase in both the intensity and extent of summer heat, particularly in central and eastern parts of the study area. The results suggest that not only have summer temperatures increased, but the area affected by extreme heat has expanded, aligning with broader signals of regional climate warming.

3.2. Case simulation assessment of S2S models

3.2.1. High temperatures in 2022

Joint data from the National Aeronautics and Space Administration (NASA) and the National Oceanic and Atmospheric Administration (NOAA) indicate that the

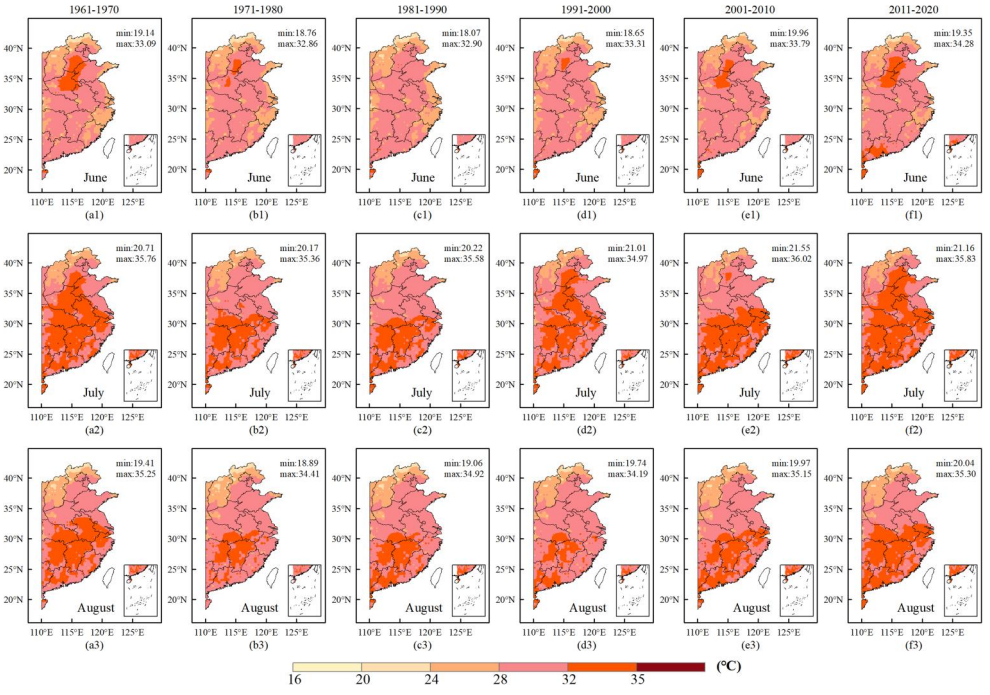

Figure 5. Distributions of decadal maximum temperature in each month from June to August.

summer of 2022 was a record-breaking season. To characterize the extreme weather conditions of that year, summer temperature anomalies in daily maximum temperatures across eastern China were calculated.

Figures 6 and 7 present the temporal variations and anomalies of the maximum, minimum, and mean daily maximum temperatures over eastern China during June to August in 2022. The maximum temperature exhibited a fluctuating upward trend throughout the summer, rising from approximately 38 °C in early June to peak around 44 °C in mid-July, then remaining consistently above 40 °C in August despite minor fluctuations. While the mean temperature persistently exceeded 30 °C, the minimum temperature also showed an overall increasing trend despite considerable variability. Anomaly analysis revealed that positive anomalies dominated all three temperature metrics: both maximum and mean temperatures showed nearly exclusively positive anomalies, while positive anomalies accounted for over 50% of days for minimum temperatures. These patterns clearly demonstrate that summer 2022 temperatures were significantly higher than climatological norms. The particularly pronounced positive anomalies in August maximum temperatures provide further evidence of the exceptionally high temperatures observed that month.

The analysis of the spatial distribution of anomalies in minimum, mean, and maximum daily maximum temperatures across eastern China during summer 2022 (Figure 8) reveals several notable patterns. The mean and maximum temperatures exhibited positive anomalies in over 95% of the study area, with particularly pronounced anomalies observed for maximum temperatures. In contrast, minimum temperatures displayed more frequent negative anomalies, consistent with previous

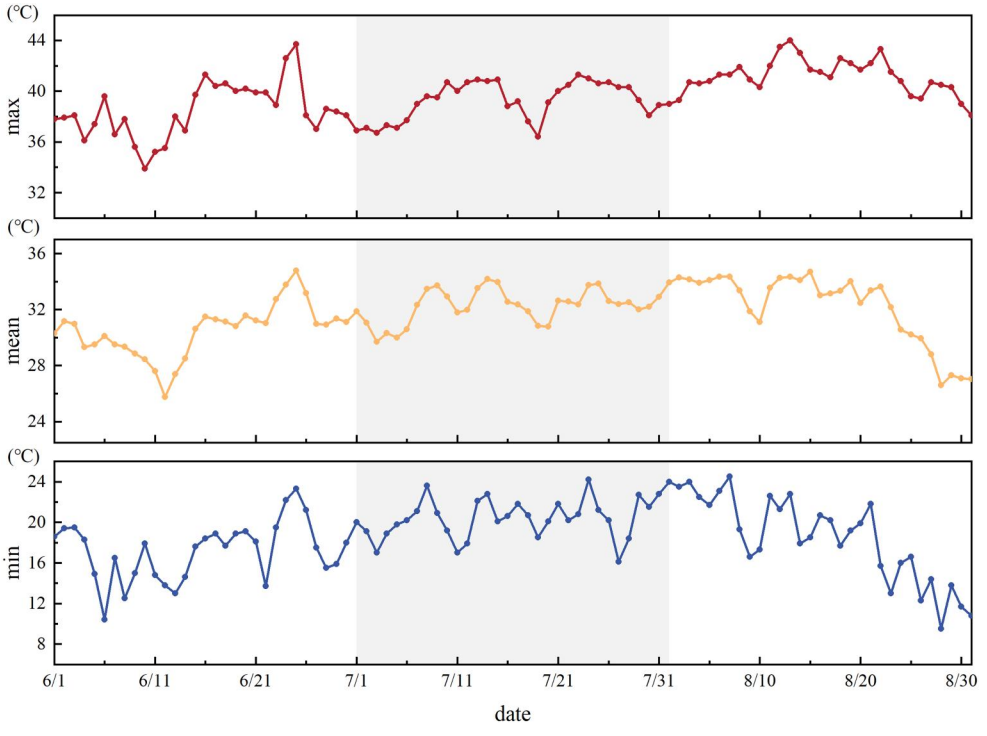

Figure 6. Minimum, mean and maximum of daily maximum temperatures in summer 2022.

findings. Notably, the central region showed a higher concentration of positive anomalies, indicating this area experienced more intense heat waves compared to climatological norms. Both temporal and spatial analyses consistently demonstrate the exceptional intensity and hazardous nature of the 2022 heat extremes.

3.2.2. Simulation assessment of S2S models

Frequent occurrences of extreme high temperature weather make it crucial for predicting timely and accurately. Sub-seasonal forecasts with effective prediction skills can provide practical information for decision-making in government and commercial sectors, as these decisions are often influenced by sub-seasonal climate variations (Yang 2008; Hu et al. 2020). In the following this study evaluated the high-temperature prediction capabilities of four operational forecasting models during summer 2022 by analyzing biases and RMSE between modeled and observed maximum temperatures across different lead times. The analysis examined forecast lead times of 1, 5, 10, 15, 20, 25, 30, 35, and 40 days. While the 15–40 day range falls within the subseasonal-to-seasonal timescale, the shorter 1–10 day forecasts were also included for comparative purposes.

Figures 9 and 10 provide a comprehensive overview of forecast biases in summer 2022 daily maximum temperature produced by four climate models—CMA, ECMWF, UKMO, and NCEP—across lead times ranging from 1 to 40 days. The intensity of the color reflects the magnitude of the bias. And RMSE values are also indicated for each model, providing a quantitative measure of forecast accuracy.

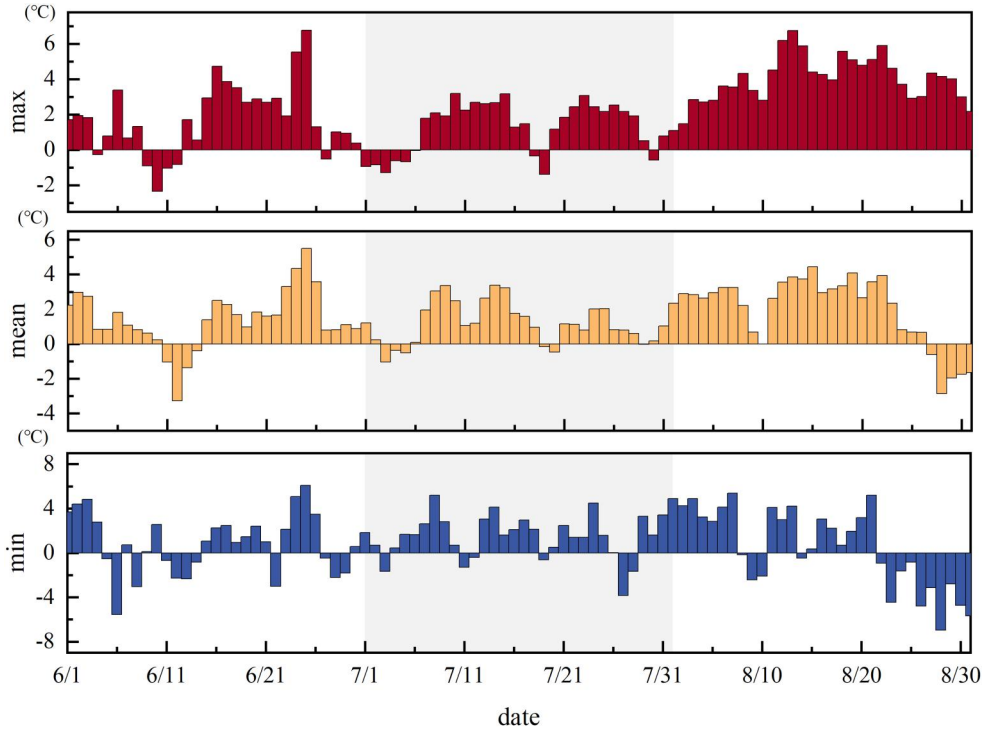

Figure 7. Anomalies in minimum, mean and maximum of daily maximum temperatures in summer 2022.

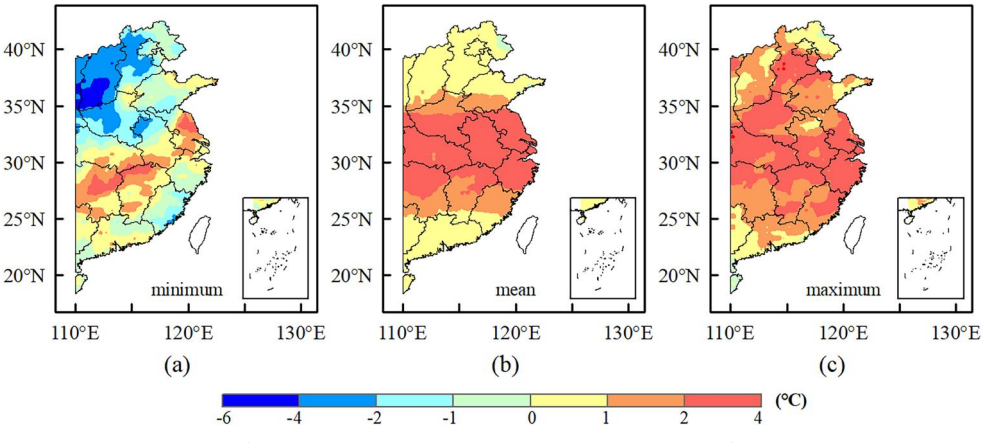

Figure 8. Distributions of anomalies in minimum, mean and maximum of daily maximum temperatures in summer 2022.

From 1 to 10-day lead times, all four models exhibit relatively low forecast errors, suggesting high accuracy in short-term forecasts. As lead time increases to 15–40 days, forecast errors gradually rise, with RMSE values increasing to around 5.5, reflecting greater uncertainty in medium- to long-range forecasts. The performance of different models varies. NCEP and CMA exhibit consistently higher RMSE values throughout the entire forecast period, indicating relatively poor performance. In contrast,

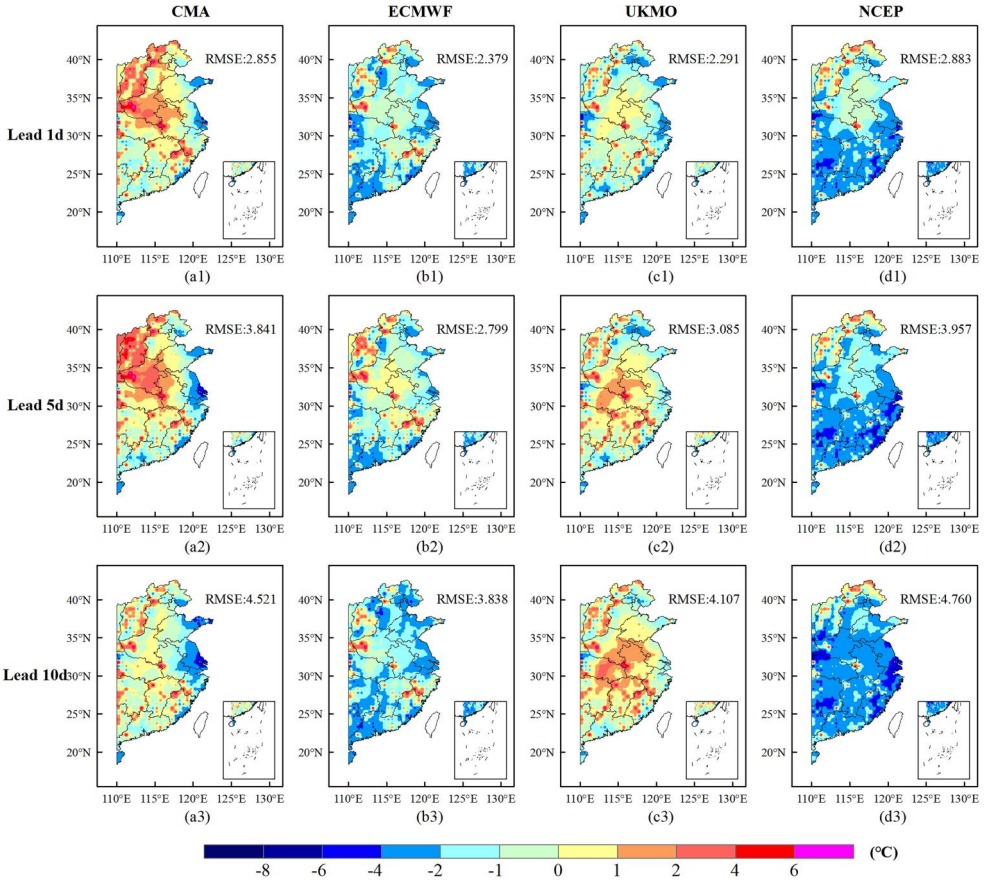

Figure 9. Biases of maximum temperature predicted by four models under the lead time of 1-day, 5-day and 10-day.

ECMWF and UKMO demonstrate lower RMSE values, with the latter excelling in short-term forecasting and the former showing superior skill at the subseasonal-to-seasonal scale. In terms of bias, distinct patterns are also observed. CMA and UKMO tend to show warm biases across most lead times, while ECMWF and NCEP exhibit more cold biases.

Overall, the results highlight the growing forecast uncertainty with increasing lead time and underscore the importance of model selection. For short-term forecasts, models such as UKMO and ECMWF demonstrate superior performance. For longer-term forecasts, increased uncertainty across all models must be accounted for.

In addition to assessing the ability of four models to simulate the maximum temperatures, this study also evaluated their performance in predicting heatwave events. Based on the heatwave definition provided in the methodology section, the 90th percentile of daily maximum temperature during the summer of 2022 was used as the threshold. Therefore two major heatwave events were identified in eastern China: from August 5 to August 7 and from August 12 to August 15.And before formal evaluation, the forecast frequency of ECMWF and CMA was converted to a daily

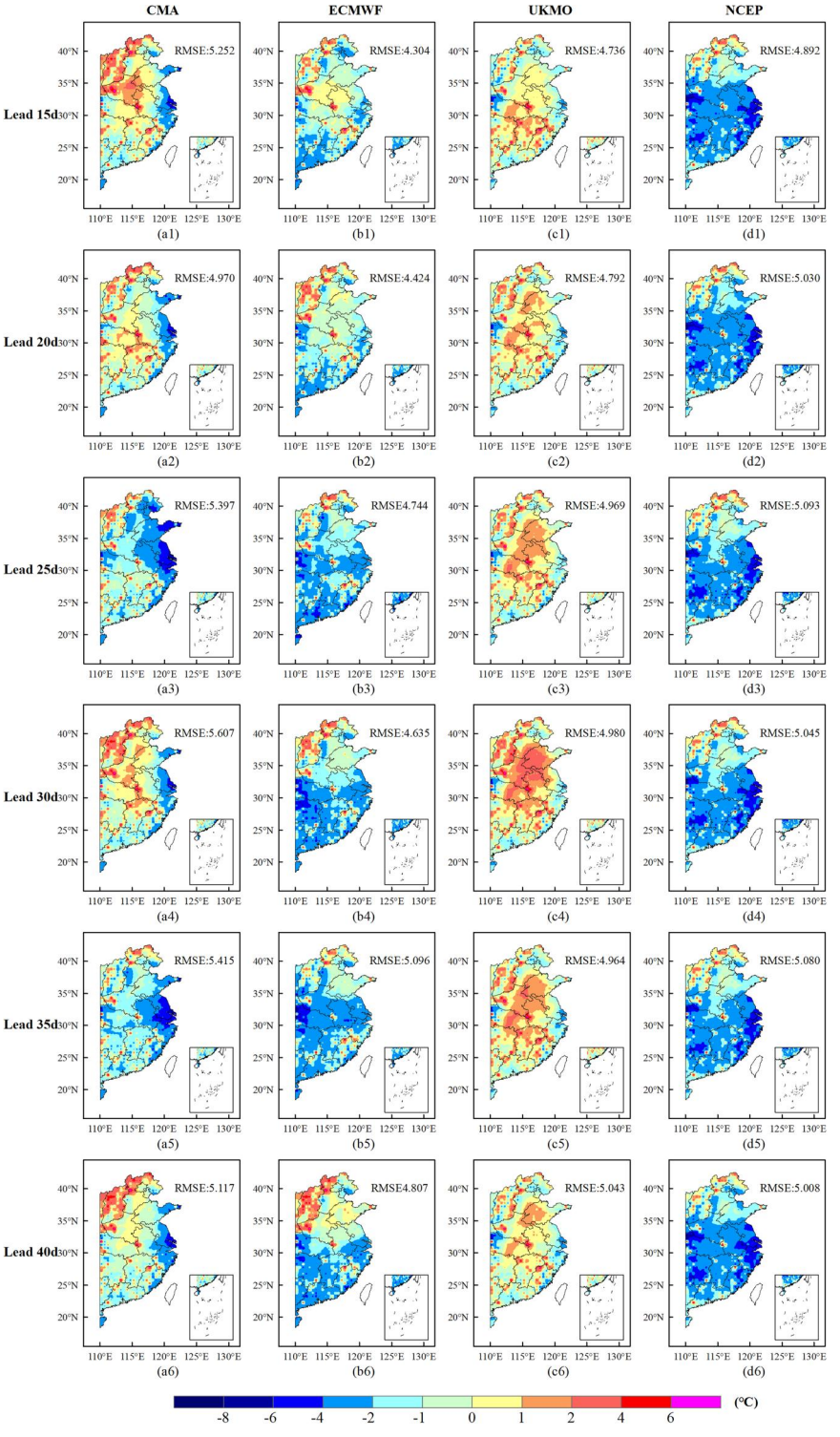

Figure 10. The same as Figure 9, but under the lead time of 15-day, 20-day, 25-day, 30-day, 35-day and 40-day.

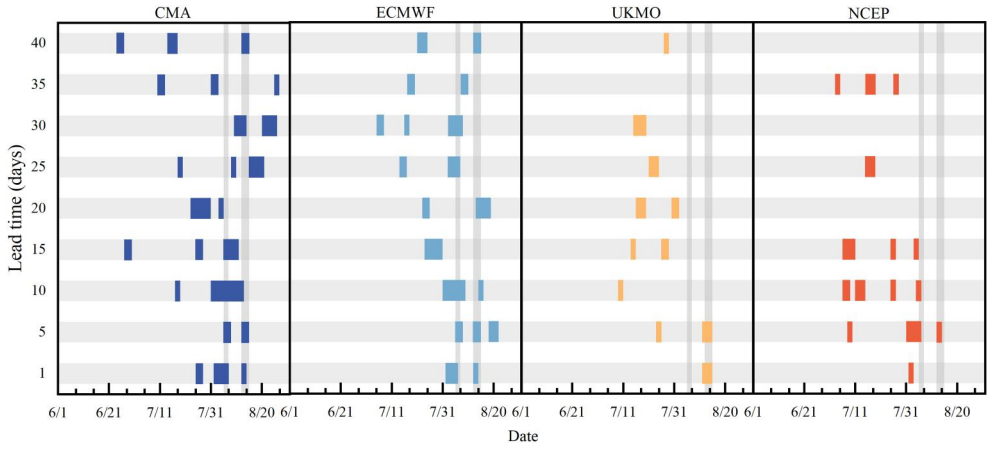

Figure 11. Occurrences of heatwaves predicted by four models in summer 2022 (the dark grey rectangle represents the observed heatwave event (August 5th to August 7th and August 12th to August 15th); the colored horizontal lines represent the periods of heatwave occurrence predicted by different models at various forecast lead times).

scale based on the data reconstruction method described earlier. Heatwave periods were then calculated individually for each of the four models.

The predictions for the 2022 summer heatwave from four models are shown in Figure 11. All four models predicted heatwaves mainly during mid-July to mid-August, with CMA additionally forecasting an earlier event in June. UKMO and NCEP predicted fewer heatwave occurrences. Notably, during the August 5–7 event, UKMO failed to capture the heatwave under any lead time, although it did predict a separate event under the 1-day and 5-day lead forecast, albeit with a one-day discrepancy. NCEP managed to capture both events under the 5-day lead forecast, but the predictions were incomplete. CMA and ECMWF detected a greater number of heatwave events across different lead times. Both models successfully forecasted the August 12–15 heatwave under 5-day and 40-day lead times, and also captured it under the 1-day lead, though the predicted duration was shorter by one day. However, neither model was able to perfectly capture the August 5–7 event. For this event, both models predicted a longer-than-observed duration, indicating a temporal bias. Notably, ECMWF was able to detect this event under the longer lead times of 25 and 30 days, suggesting its potential skill in capturing heatwaves at extended forecast ranges, albeit with timing inaccuracies.

The results reveal considerable differences in the models' ability to predict the timing of heatwave occurrences. Each model exhibits unique strengths and limitations depending on the forecast range. Selecting an appropriate model is therefore crucial for improving the accuracy of heatwave prediction, especially in the context of early warning and risk management.

Finally, the calculation of the relevant indicators for this evaluation are shown in Figure 12, providing a more comprehensive understanding of the results. Regarding spatial correlation (Figure 12a), UKMO demonstrates the highest spatial similarity in simulated daily maximum temperature after a 20-day lead time, while ECMWF performs best at shorter lead times. CMA, however, consistently shows lower spatial

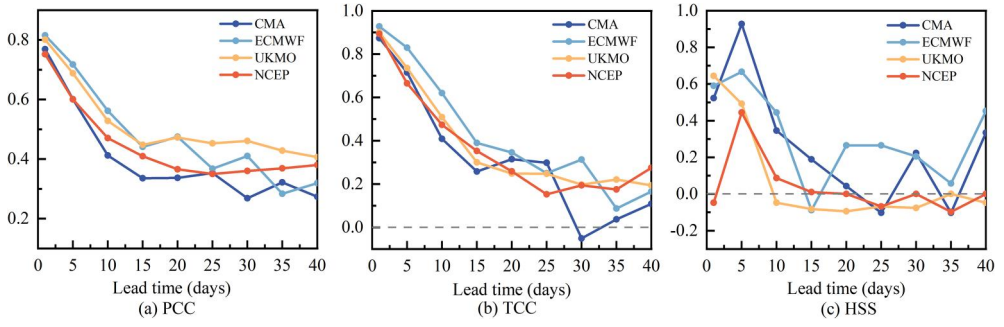

Figure 12. (a) PCC, (b) TCC, and (c) HSS of four models.

correlation throughout the forecast period. These results indicate that UKMO and ECMWF are better at capturing the spatial distribution characteristics of temperature over the study region. Regarding the temporal correlation coefficient (Figure 12b), ECMWF achieves the highest similarity in the temporal evolution of daily maximum temperatures during most of the study period, though this performance declines at 35-day and 40-day lead times. CMA reaches its peak temporal correlation at a 25-day lead time, but the correlation turns negative at 30 days. These findings suggest that the models differ in their ability to represent temporal evolution across various forecast horizons, and that appropriate lead times should be chosen based on the specific application. Finally, the Heidke Skill Score (HSS) for heatwave prediction shows that all four models achieve relatively high HSS values at the 5-day lead time, indicating good predictive skill for both heatwave events. CMA exhibits the highest precision among the models in this timeframe. Overall, ECMWF and CMA consistently outperform the other two models, with ECMWF showing improved skill as the lead time increases.

4. Conclusion and discussion

After conducting a temporal and spatial analysis of the maximum temperature in the region east of 110°E in China (excluding Inner Mongolia and the Northeast) from 1961 to 2020, the typical extreme weather year of 2022 was selected as a case study to explore the ability of high temperature and heatwave prediction of four S2S models. The following conclusions are drawn:

From 1961 to 2020, daily maximum temperatures during summer months (June–August) in China exhibited a clear warming trend across minimum, mean, and maximum values. The minimum temperature increased by more than 2 °C, with all three metrics rising most notably during the 2011–2020 period. Spatially, high-temperature zones expanded steadily, particularly in central and eastern regions, reflecting a broader intensification and spatial extension of extreme heat, consistent with the ongoing trend of regional climate warming.

The short-term forecasts (1–10 days) generally exhibit low bias and RMSE, while forecast errors increase with longer lead times. ECMWF and UKMO showed superior performance in terms of RMSE, with UKMO performing best at shorter lead times

and ECMWF demonstrating better skill at the subseasonal-to-seasonal scale. CMA and NCEP consistently showed higher RMSE and weaker spatial correlation.

For heatwave prediction, CMA and ECMWF successfully captured key events at multiple lead times, particularly the August 12–15 event. However, neither model fully captured the August 5–7 heatwave without temporal bias. UKMO and NCEP predicted fewer events, with UKMO failing to detect the August 5–7 event at any lead time. Skill score evaluation using HSS shows that all models performed well at a 5-day lead, with CMA achieving the highest precision.

This study provides a detailed examination of the temporal and spatial variations in the minimum, average, and maximum temperatures over Eastern China from 1961 to 2020. Additionally, it offers a preliminary understanding of the predictive performance of four operational centers participating in the Sub-seasonal to Seasonal (S2S) prediction project. However, the physical mechanisms underlying the formation of high temperature weather are highly complex. Further investigation is needed to understand the inherent connections among the three temperature variables, as well as the causes of the deviations in model predictions and the key factors influencing the accuracy of heatwave forecasts.

Author contributions

CRediT: **Xuemin Shen**: Conceptualization, Formal analysis, Investigation, Visualization, Writing – original draft; **Aixia Feng**: Conceptualization, Data curation, Supervision, Writing – review & editing; **Changgui Gu**: Supervision, Writing – review & editing; **Qiguang Wang**: Conceptualization, Data curation, Supervision, Writing – review & editing.

Disclosure statement

No potential conflict of interest was reported by the author(s).

Funding

This work was supported by the National Natural Science Foundation of China under grant numbers U2342211, Grants 41975100 and 12275179, the Natural Science Foundation of Shanghai, China (Grant No. 21ZR1443900), and the Joint Research Project for Meteorological Capacity Improvement (Grant No.22NLTSZ004).

Data availability statement

The Chinese daily surface temperature dataset (V2.0, $0.5^\circ \times 0.5^\circ$) are available from the corresponding author on reasonable request. The S2S model dataset are available at ECMWF | S2S, ECMWF, Realtime, Daily averaged.

References

Alexander LV, Zhang X, Peterson TC, Caesar J, Gleason B, Klein Tank AM, Haylock M, Collins D, Trewin B, Rahimzadeh F, et al. 2006. Global observed changes in daily climate extremes of temperature and precipitation. J Geophys Res. 111(D5) doi: 10.1029/2005JD006290.

Ding T, Qian WH. 2011. Geographical patterns and temporal variations of regional dry and wet heatwave events in China during 1960-2008. Adv Atmos Sci. 28(2):322–337. doi: 10.1007/s00376-010-9236-7.

Ding T, Qian WH, Yan ZW. 2010. Changes in hot days and heat waves in China during 1961–2007. Int J Climatol. 30(10):1452–1462. doi: 10.1002/joc.1989.

Dong XY, Wu BY. 2019. Dynamic linkages between heat wave events in Jianghuai Region and Arctic summer cold anomaly. J Appl Meteorol Sci. 30(4):431–442. Chinese.

He HR. 2020. Evaluation and error correction of subseasonal summer precipitation hindcast over Eastern China in ECMWF S2S database [master's thesis]. Nanjing: Nanjing University of Information Science and Technology. Chinese.

Heidke P. 1926. Berechnung des Erfolges und der Güte der Windstärkevorhersagen im Sturmwarnungsdienst. Geogr Ann. 8(4):301–349.

Hu X, Zhang ZQ, Zhang Q, Wang J. 2020. Analysis and application of sub-seasonal to seasonal prediction data. J Meteorol Sci. 48(6):779–787. Chinese.

Jiang XF. 2021. Future risk assessment and the impact on electricity consumption of extreme high temperature events in Eastern China [master's thesis]. Nanjing: Nanjing University of Information Science and Technology. Chinese.

Lin X, Guan ZY. 2008. Temporal-spatial characters and interannual variations of summer high temperature in Eat China. Trans Atmos Sci. 31(1):1–9. Chinese.

Li SS, Yang SN, Zhang DH, Liu XF. 2015. Spatiotemporal variability of heat waves in Beijing-Tianjin-Hebei Region and influencing factors in recent 54 years. J Appl Meteorol Sci. 26(5):545–554. Chinese.

Long Y. 2022. Predictability of spatial distribution of extreme high temperature days in Eastern China during summer [master's thesis]. Nanjing: Nanjing University of Information Science and Technology. Chinese.

Lu CH, Shen YC, Li YH, Xiang B, Qin YJ. 2022. Role of intraseasonal oscillation in a compound drought and heat event over the middle of the Yangtze River Basin during midsummer 2018. J Meteorol Res. 36(4):643–657. doi: 10.1007/s13351-022-2008-3.

Perkins SE. 2015. A review on the scientific understanding of heatwaves—Their measurement, driving mechanisms, and changes at the global scale. Atmos Res. 164–165:242–267. doi: 10.1016/j.atmosres.2015.05.014.

Perkins SE, Alexander LV, Nairn JR. 2012. Increasing frequency, intensity and duration of observed global heatwaves and warm spells. Geophys Res Lett. 39(20) doi: 10.1029/2012GL053361.

Perkins SE, Lewis SC. 2020. Increasing trends in regional heatwaves. Nat Commun. 11(1):3357. doi: 10.1038/s41467-020-16970-7.

Qi X, Yang J. 2019. Extended-range prediction of a heat wave event over the Yangtze River Valley: role of intraseasonal signals. Atmos Ocean Sci Lett. 12(6):451–457.

Shi HB. 2012. Climatic characteristics and the spatio-temporal variation of high temperature days in North China. Sci Geogr Sin. 32(07):866–871. Chinese.

Stefanon M, D' Andrea F, Drobinski P. 2012. Heatwave classification over Europe and the Mediterranean region. Environ Res Lett. 7(1):014023. doi: 10.1088/1748-9326/7/1/014023.

Sun JQ, Wang HJ, Yuan W. 2011. Decadal variability of the extreme hot event in China and its association with atmospheric circulations. Clim Environ Res. 16(2):199–208. Chinese.

Sun Y, Zhang XB, Zwiers FW, Song LC, Wan H, Hu T, Yin H, Ren GY. 2014. Rapid increase in the risk of extreme summer heat in Eastern China. Nature Clim Change. 4(12):1082–1085. doi: 10.1038/nclimate2410.

Wang Y. 2020. Response of summer high temperatures in Eastern China's urban agglomerations to future global warming [master's thesis]. Nanjing: Nanjing University of Information Science and Technology. Chinese.

Wang C, Li JP. 2022. Evaluation of summer daily precipitation forecast over eastern China based on subseasonal to seasonal (S2S) models. J Mar Meteorol. 42(4):22–36. Chinese.

Xie JH. 2021. Evaluation and correction of heatwaves forecast in the Yangtze River Basin Based on Subseasonal-to-Seasonal (S2S) prediction models [master's thesis]. Nanjing: Nanjing University of Information Science and Technology. Chinese.

Xie JH, Yu JH, Chen HS, Hsu PC. 2020. Sources of subseasonal prediction skill for heatwaves over the Yangtze River Basin revealed from three S2S models. Adv Atmos Sci. 37(12):1435–1450. doi: 10.1007/s00376-020-0144-1.

Yang QM. 2008. Extended-range weather forecasting for 10-30 days and development trends. New Technol New Prod China (7):96–97. Chinese.

Yang J, Zhu T, Gao MN, Lin H, Wang B, Bao Q. 2018. Late-July barrier for subseasonal forecast of summer daily maximum temperature over Yangtze River Basin. Geophys Res Lett. 45(22):12–610. 12,615. doi: 10.1029/2018GL080963.

Yu ET, Sun JQ. 2019. Extreme temperature projection over northwestern China based on multiple regional climate models. Trans Atmos Sci. 42(1):46–57. Chinese.

Zhai PM, Pan XH. 2003. Change in extreme temperature and precipitation over northern China during the second half of the 20th century. Acta Geophys Sin. 58(Suppl I):1–10. Chinese.

Zhang GW. 2021. Spatial-temporal characteristics of heatwaves with related possible causes and future heat risk projections in North China [dissertation]. Nanjing: Nanjing University of Information Science and Technology. Chinese.

Zhu ZP, Fan YF. 2009. The analysis of the character of summer heat wave over Eastern China and its prediction. Atmos Sci Res Appl. (2):69–75. Chinese.